Induced Sheath Voltage Investigation under Normal and Fault Conditions for Practical Underground Cable System

Thanapong Suwanasri[1,*], Phanupong Fuangpian[1], Nattapon Punmala[1], Sangay Wangdi[1] and Cattareeya Suwanasri[2]

[1]Department of Electrical and Software Systems Engineering,
The Sirindhorn International Thai-German Graduate School of Engineering
[2]Department of Electrical and Computer Engineering, Faculty of Engineering,
King Mongkut's University of Technology North Bangkok,
1518 Pracharat 1 Rd., Wongsawang, Bangsue, Bangkok, Thailand

Abstract: This paper presents a numerical calculation and simulation model to investigate the induced sheath voltage of a 115 kV underground cable system influenced by magnetic induction of its neighboring feeders and by fault condition. The simulation model developed in the ATP/EMTP program was used for such investigation. Actual data acquired from all the equipment or derived from physical dimension of equipment was employed as input parameters in the simulation model. Different cases of power cable installation as single feeder with load, double feeders with load sharing, and double feeders with double load current as well as under three phase and single line to ground fault had been considered in this work. Then, the induced sheath voltage was investigated with the practical cable system installed in a power plant to customer. The investigation included single point bonding, both-side bonding with cross bonding at joints in the manhole. The results showed the voltage rise of induced sheath voltage in case of three phase and single line to ground fault, while this severity could be minimized by the appropriate bonding technique.

Keywords— Induced sheath voltage, Cross bonding, Single point bonding, Both-side bonding, Underground cable, ATP-EMTP

I. INTRODUCTION

Currently, power distribution system has been widely expanded to support a tremendous increase in electricity consumption in industrial estates, which is of prime concern for service providers of electric power business. This leads to a new construction of power stations and underground cable feeder installation to increase the performance and capacity of power delivery system while maintain electricity supply stability and reliability [1-2]. In underground cable system, various methods on cable bonding practice [3-4] as well as metallic earthing system have been employed to reduce sheath voltage to a safe level as well as to control the circulating current in the earthing system [5-7], which could lead to shock hazard, overheat in cable insulation and reduction in power transmission capacity [8-9]. This affects the system stability and safety of maintenance engineer. Moreover, these sheath voltage and circulating current in cable earthing system are important factors for condition assessment of underground cable system [10-11]. Sometimes, both simulation technique and field testing have been performed to investigate such phenomena in the system [12-13]. Therefore, this paper presents an understanding of induced sheath voltage on metallic shield of multiple circuits of underground cable arising mainly from induced magnetic field caused by electric current flowing in conductors. This work presents the investigation of induced sheath voltage of an underground cable system with cross bonding at joints in manhole and bonded at each end of the sheath as single point bonding and both-side bonding. A single feeder influenced by magnetic induction by multiple circuits of 115 kV underground cable feeders in the vicinity and under fault condition were also investigated.

II. INDUCED SHEATH VOLTAGE CALCULATION

The design of grounded cable shield and induced sheath voltage calculation of underground cable were explained in this section.

The manuscript received June 7,2021; revised June 14, 2021; accepted June 24, 2021. Date of publication June 30, 2021.

*Corresponding author: Thanapong Suwanasri, Department of Electrical and Software Systems Engineering, the Sirindhorn International Thai-German Graduate School of Engineering, King Mongkut's University of Technology North Bangkok, Thailand. (E-mail: thanapong.s.epe@tggs-bangkok.org).

A. Induced Sheath Voltage for Single Circuit

From ANSI/IEEE Std. 575-1988, general equation for sheath voltage calculation of any cable formation was expressed in Eq. (1).

$$\begin{aligned}\bar{e}_a &= j\omega I_a \times (2\times10^{-7}) \times \left[-\frac{1}{2}\ln\left(\frac{2S_{ab}^2}{d\times S_{ac}}\right) + j\frac{\sqrt{3}}{2}\ln\left(\frac{2S_{ac}}{d}\right)\right] \\ \bar{e}_b &= j\omega I_b \times (2\times10^{-7}) \times \left[\frac{1}{2}\ln\left(\frac{4S_{ab}\times S_{bc}}{d^2}\right) + j\frac{\sqrt{3}}{2}\ln\left(\frac{S_{bc}}{S_{ab}}\right)\right] \\ \bar{e}_c &= j\omega I_c \times (2\times10^{-7}) \times \left[-\frac{1}{2}\ln\left(\frac{2S_{bc}^2}{d\times S_{ac}}\right) - j\frac{\sqrt{3}}{2}\ln\left(\frac{2S_{ac}}{d}\right)\right]\end{aligned} \quad (1)$$

where I_a, I_b, and I_c are phase currents in major circuit, d is a geometric mean sheath diameter (arithmetic mean), S_{ab}, S_{bc}, and $S_{ac}$are axial spacing between phases.

B. Induced Sheath voltage for multiple circuit

From ANSI/IEEE Std. 575 – 2014 [2], general equations for sheath voltage calculation of double-circuit systems were expressed in Eqs. (2)-(4), where S_{12} is distance from cables 1 to 2 and R_{sm} is mean sheath radius. The cable installation structure with cross-bonding technique were presented in Fig. 1. The layout of underground cables installed in a duct bank was shown in Fig. 2 while a single core cable construction and its dimension were given in Fig. 3.

$$\begin{aligned}\bar{e}_a &= I_a\times jX_{aa} + I_b\times jX_{ab} + I_c\times jX_{ac} \\ \bar{e}_b &= I_a\times jX_{ab} + I_b\times jX_{bb} + I_c\times jX_{bc} \\ \bar{e}_c &= I_a\times jX_{ac} + I_b\times jX_{bc} + I_c\times jX_{cc}\end{aligned} \quad (2)$$

$$\begin{aligned}X_{aa} &= 1.257\times f\times10^{-6}\ln\left(1/\left(r_{sm}\times S_{14}\right)\right) \\ X_{bb} &= 1.257\times f\times10^{-6}\ln\left(1/\left(r_{sm}\times S_{25}\right)\right) \\ X_{cc} &= 1.257\times f\times10^{-6}\ln\left(1/\left(r_{sm}\times S_{36}\right)\right)\end{aligned} \quad (3)$$

$$\begin{aligned}X_{ab} &= 1.257\times f\times10^{-6}\ln\left(1/\left(S_{12}\times S_{15}\right)\right) \\ X_{bc} &= 1.257\times f\times10^{-6}\ln\left(1/\left(S_{23}\times S_{35}\right)\right) \\ X_{ac} &= 1.257\times f\times10^{-6}\ln\left(1/\left(S_{13}\times S_{16}\right)\right)\end{aligned} \quad (4)$$

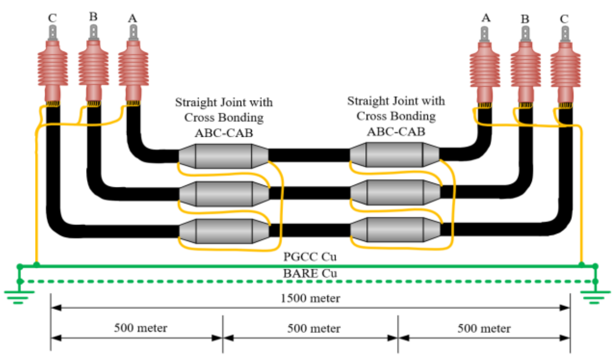

Fig. 1. Cable installation structure with cross-bonding.

The actual parameters of a single core 115 kV underground cable and the required parameters for simulation model in the ATP/EMTP program were presented in Tables I and II.

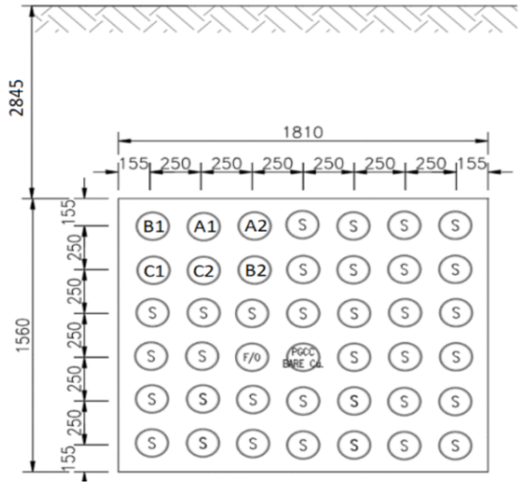

Fig. 2. Cable installation layout in duct bank.

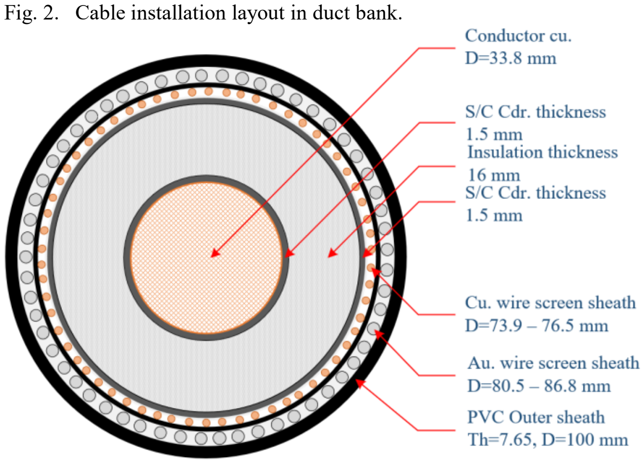

Fig. 3. Single core cable construction and its dimension.

TABLE I.
PARAMETERS OF SINGLE CORE CABLE IN ATP/EMTP

115 kV CU/XLPE/CWS/LAT/AWA/PVC Single core 800 sq.mm	Data	Core	Sheath	Armor
Model Type	PI		N/A	
#Ph	11			
Number of cables	5			
Cable installed location	ground			
The ground resistivity in ohm*m (Rho)	100			
System Line/Cable Data	single core cable			
Inner radius of conductor [m] (Rin)	N/A	0.000000	0.03695	0.040250
Outer radius of conductor [m] (Rout)		0.016900	0.038250	0.043400
Resistivity of the conductor material (Rho)		1.68E-08	1.68E-08	2.65E-08
Relative permeability of the conductor material (mu)		0.999994	0.999994	1.000022
Relative permeability of the insulator material outside the conductor (mu of ins)		1	1	1
Relative permittivity of the insulator material outside the conductor (eps of ins)		2.3	1	1
Thickness of inner semiconductor layer in [m]		0.0015	0	0
Thickness of outer semiconductor layer in [m]		0.0015	0	0

TABLE II.
ATP/EMTP PARAMETER FOR SINGLE CORE 115 KV CABLE

Model	Parameter
Current source	Amplitude L-G rms : 250/500 A System frequency : 50 Hz Phase angle : 0 degree Start time : -1 sec Stop time : 100 sec
Cross-bond	Transposed ABC-CAB
Load	Simulated load R_1(Ohms): 1 L_1(mH): 0 C_1(uF): 0
142∠0 Current probe	No. of phases: 1 or 3 phases Monitor: 3 phases
13∠-98 Voltage probe	No. of phases: 1 or 3 phases Monitor: 3 phases
I2MH2-IU6MH1 LCC 288. m LCC cable model	Name: Cable name Type: Single core cable Cable in: Ground Model: PI model No. of phase: count from number of cable (6) including sheath of each phase (3) Standard data: Rho: 100 ohm*m Freq. int: 50 Hz Length: cable length in each section Model type: PI

III. SIMULATION MODELS

Three different cases were simulated as examples. Case 1 was single feeder with single load. Case 2 was double feeders with load sharing. Case 3 was double feeders with double load current. The diagrams and their developed circuits in ATPDraw program of such three cases were shown in Figs. 4-6 and Figs. 7-9, respectively.

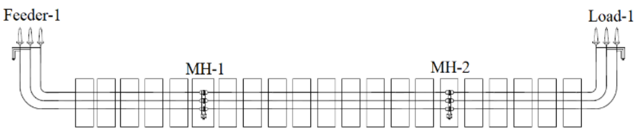

Fig. 4. Diagram of single feeder with single load.

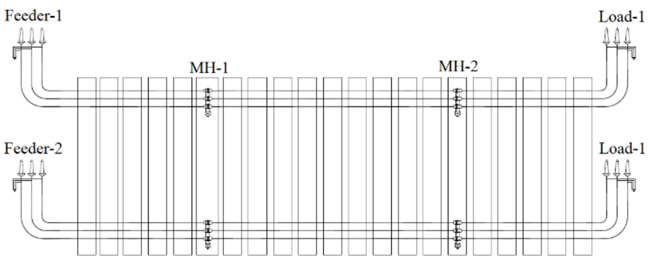

Fig. 5. Diagram of double feeders with load sharing.

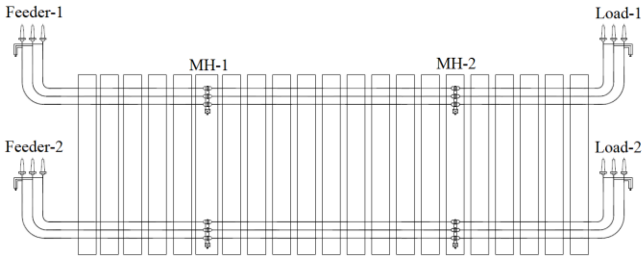

Fig. 6. Diagram of double feeders with double load current.

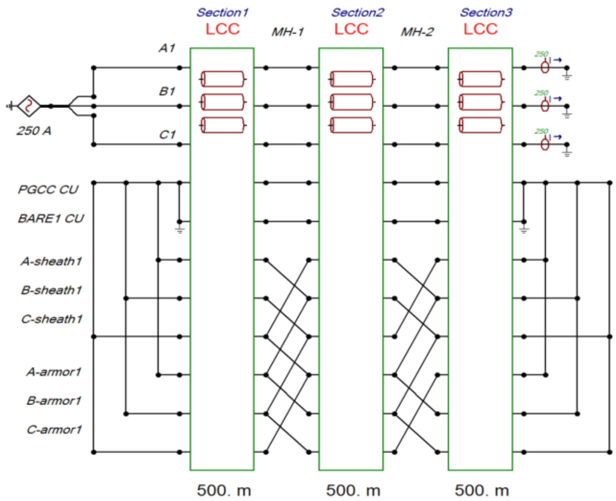

Fig. 7. Circuit diagram in ATPDraw for single feder with single load.

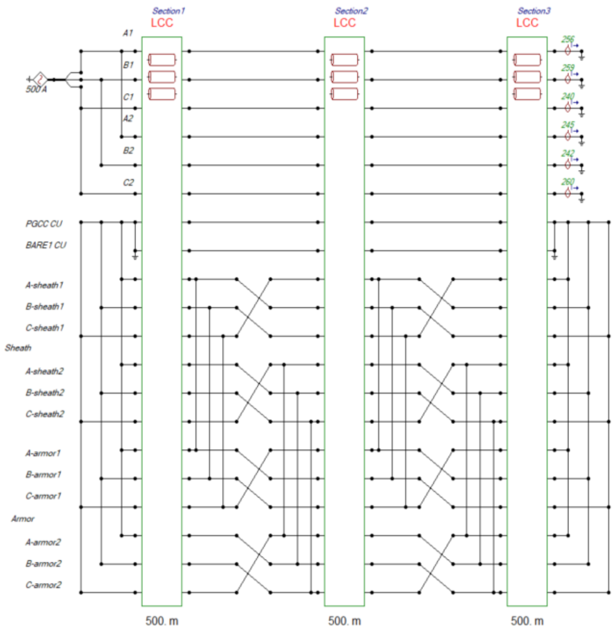

Fig. 8. Circuit diagram in ATPDraw for double feeders with load sharing.

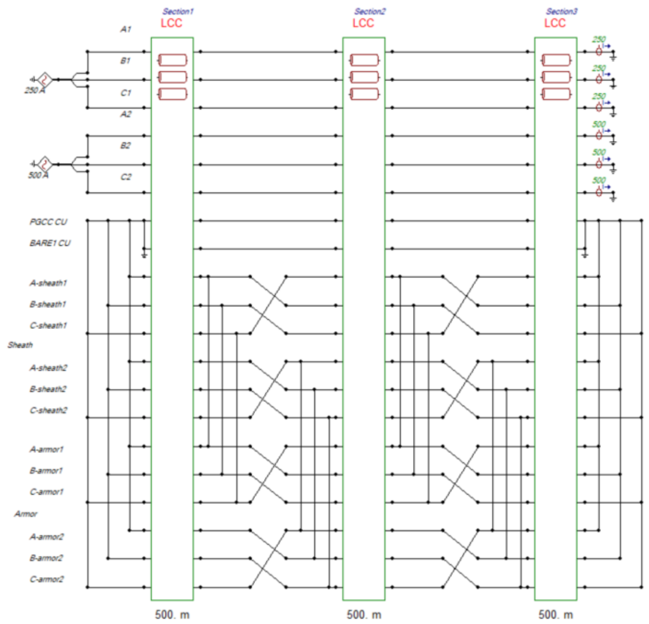

Fig. 9. Circuit diagram in ATPDraw for double feeders with double load current.

IV. Numerical and Simulation Results

The metallic sheath earthing system of such three cases has been classified as three major cases, which were single point bonding, both-side bonding and lastly induced sheath voltage investigation of practical feeder under normal and fault conditions.

A. Single Point Bonding

The induced sheath voltages of phase A, B, and C had been calculated according to the theory in the IEEE standards and subsequently compared with the simulation result as presented in Tables III-V with a good agreement between both methods as approximately 3% deviation. After a successful verification, the simulation results of induced sheath voltage along the length of underground cable were plotted in Fig. 9-12 for those three studied cases.

TABLE III.
Comparison of Induced Sheath Voltages Between Theoretical Calculation and Simulation For Single Feeder

Source Current	Phase	Current (A)	Simulated Sheath Voltage (V/m)	Calculated Sheath Voltage (V/m) Using Eq. (1)	%Div.
250 A	A1	250	0.032817	0.031949	2.71%
	B1	250	0.029758	0.028876	3.05%
	C1	250	0.032822	0.031949	2.73%

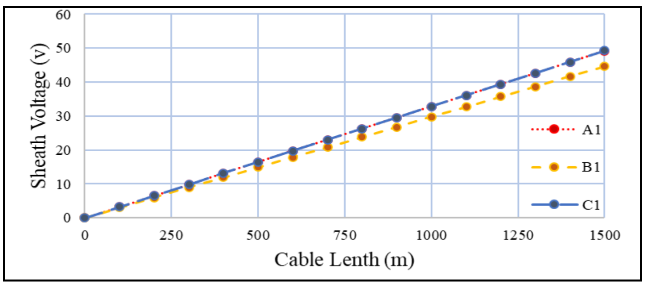

Fig. 10. Induced sheath voltages of single feeder with single load.

TABLE IV.
Comparison of Induced Sheath Voltages Between Theoretical Calculation and Simulation For Double Feeders with Load Shearing

Source Current	Phase	Current (A)	Simulated Sheath Voltage (V/m)	Calculated Sheath Voltage (V/m) Using Eq. (1)	%Div.
500 A	A1	263	0.037733	0.034389	9.72%
	B1	248	0.025093	0.024956	0.54%
	C1	238	0.040864	0.037300	9.55%
	A2	237	0.040407	0.034389	17.49%
	B2	252	0.025616	0.024956	2.64%
	C2	264	0.037381	0.037300	0.22%

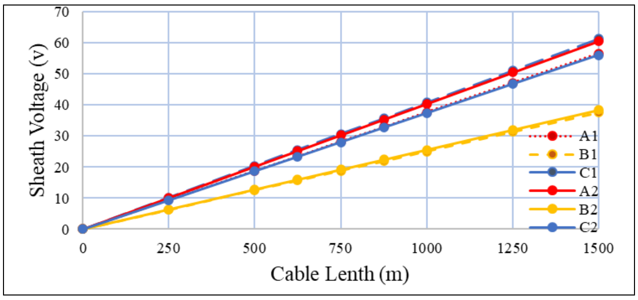

Fig. 11. Induced sheath voltages of double feeders with load shearing.

TABLE V.
Comparison of Induced Sheath Voltages Between Theoretical Calculation and Simulation For Double Feeders with Double Load Current

Source Current	Phase	Current (A)	Simulated Sheath Voltage (V/m)	Calculated Sheath Voltage (V/m) Using Eq. (1)	%Div.
250 A	A1	250	0.038201	0.031949	19.56%
	B1	250	0.022864	0.028876	20.82%
	C1	250	0.056543	0.031949	76.97%
500 A	A2	500	0.077493	0.063898	21.27%
	B2	500	0.055249	0.057754	4.33%
	C2	500	0.067845	0.063898	6.17%

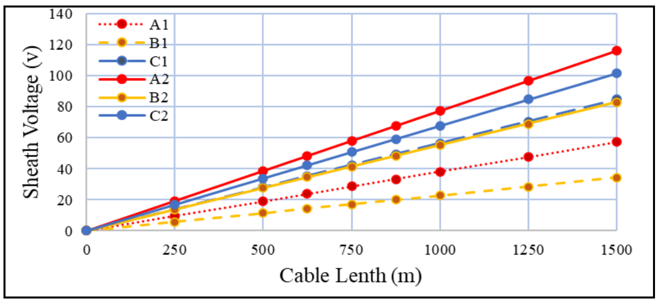

Fig. 12. Induced sheath voltages of double feeders with double load current.

It was clearly seen from the above figures that the induced sheath voltage increased with the cable length for single point bonding. The highest sheath voltage was at the open-end and it should be limit to be less than 60 V according to the safety practice in a distribution utility in Thailand. However, the safe limit of this induced sheath voltage may be differed from utility to utility or country to country. Additionally, the higher current flowing in the conductor, the higher induced sheath voltage could be expected as shown in Fig. 12.

B. Both-side Bonding

According to diagram in Fig. 5 and simulation circuit in Fig. 8, the results of induced sheath voltage of phases A, B, and C along the cable length in case of single feeder with single load of 250 were shown in Table VI and Fig. 13. The highest sheath voltages, occurring at the cross bonding point at cable joint in manhole, were approximately 16 volts at the lengths 500 in phase A and 1000 m in phase B, which was lower than 50 V in case of single point bonding and within the aforementioned safe limit of 60 V.

TABLE VI.
INDUCED SHEATH VOLTAGES ALONG CABLE LENGTH OF SINGLE FEEDER WITH SINGLE LOAD

Location (m)	Sheath Voltage (Vrms)		
	A1	B1	C1
0	0.000	0.000	0.000
250	8.117	6.687	8.109
500	16.233	13.375	16.219
750	14.784	12.614	12.454
1000	16.219	16.662	13.375
1250	8.109	8.331	6.687
1500	0.000	0.000	0.000

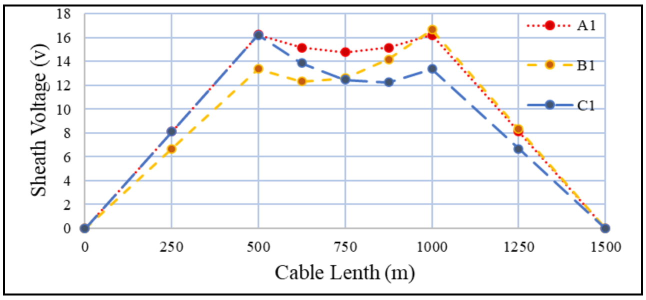

Fig. 13. Induced sheath voltages of single feeder with single load.

Case 2 was the double feeders with load sharing, whereas case 3 was double feeders with double load current. The details of load sharing current and double of load current from 250 A to 500 A were given in Table VII.

TABLE VII.
LOAD CURRENT SHARING (CASES 2) AND DOUBLE OF LOAD CURRENT (CASE 3)

Case 2			Case 3		
Load	Phase	Current (A)	Load	Phase	Current (A)
Load 1 500 A	A1	**263**	Load 1 250 A	A1	250
	B1	248		B1	250
	C1	238		C1	250
	A2	**237**	Load 2 500 A	A2	500
	B2	252		B2	500
	C2	264		C2	500

In Table VIII and Fig. 14, the results showed that the induced sheath voltages of six phases were different because of different location of cables according to installation layout in Fig. 2. This led to slightly unbalanced current in those six phases as phase A1 increased to 263 A, phase A2 reduced to 237 A etc. Therefore, the maximum induced sheath voltage approximately 18 V was found at the cross-bonding point, which is within the safety limit of 60 V.

TABLE VIII.
INDUCED SHEATH VOLTAGES ALONG CABLE LENGTH OF DOUBLE FEEDERS WITH LOAD SHEARING

Location	Sheath Voltage (Vrms)					
(m)	A1	B1	C1	A2	B2	C2
0	0.000	0.000	0.000	0.000	0.000	0.000
250	9.032	6.813	9.241	9.181	6.750	9.054
500	18.064	**13.626**	18.482	**18.362**	13.500	18.107
750	16.957	13.061	13.493	16.940	13.332	13.068
1000	**18.483**	18.063	13.626	18.108	18.362	13.501
1250	9.241	9.031	6.813	9.054	9.181	6.750
1500	0.000	0.000	0.000	0.000	0.000	0.000

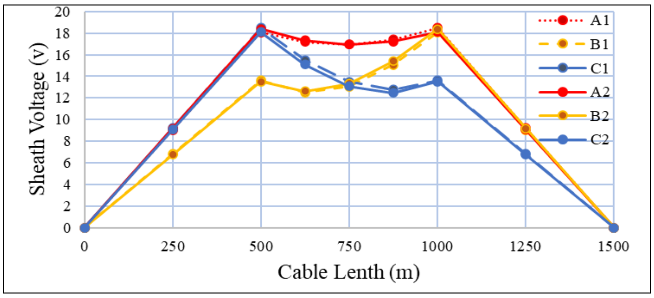

Fig. 14. Induced sheath voltage of double feeders with load sharing.

In Case 3, feeder 2 was assigned to carry double of load current as 500 A compared with feeder 1 as 250 A. In Table IX and Fig. 15, the higher current in feeder 2 affected to the higher induced sheath voltage in its own phases as 34.814 V, which is about 1.89 times greater than its usual operation as 18 V at 250 A. Moreover, this higher current in feeder 2 could mutually induced the slightly increasing induced sheath voltage of feeder 1 from 18.5 V to 21.3 V.

TABLE IX.
INDUCED SHEATH VOLTAGES ALONG CABLE LENGTH OF DOUBLE FEEDERS WITH DOUBLE LOAD CURRENT

Location	Sheath Voltage (Vrms)					
(m)	A1	B1	C1	A2	B2	C2
0	0.000	0.000	0.000	0.000	0.000	0.000
250	10.031	7.121	10.644	17.407	13.267	16.722
500	20.062	14.242	21.288	**34.814**	26.534	33.444
750	19.420	13.761	15.070	31.452	26.046	24.664
1000	**21.288**	20.062	14.242	33.445	34.814	26.534
1250	10.644	10.031	7.121	16.722	17.047	13.267
1500	0.000	0.000	0.000	0.000	0.000	0.000

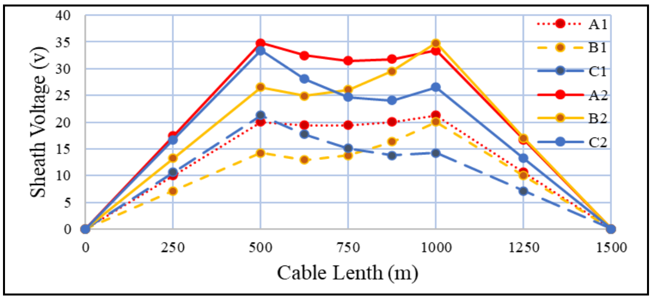

Fig. 15. Induced sheath voltages of double feeders with double load current.

C. Induced sheath voltage investigation of practical feeder under normal and fault conditions

After a successful verification of the simulation model and analytical method in the previous section, the simulation model with cross bonding at joints in the manhole and the actual data of cable and installation layout in a power producer was developed and shown in Fig. 16. The ATP/EMTP simulation circuit was used to demonstrate the investigation of induced sheath voltage of a 1,627 m long cable with two cross bonding points under normal operation and short circuit conditions. The sheath of cable was grounded at both sides to generating plant ground grid modeled as 1 Ohm grounding resistance and customer's substation ground grid modeled as 2 Ohm grounding resistance. Four cases were studied to demonstrate the induced sheath voltage in cable circuit including 1) cable with normal operation, 2) three phase faults, 3) cable with internal single-line-to-ground fault, and 4) cable with external single-line-to-ground fault.

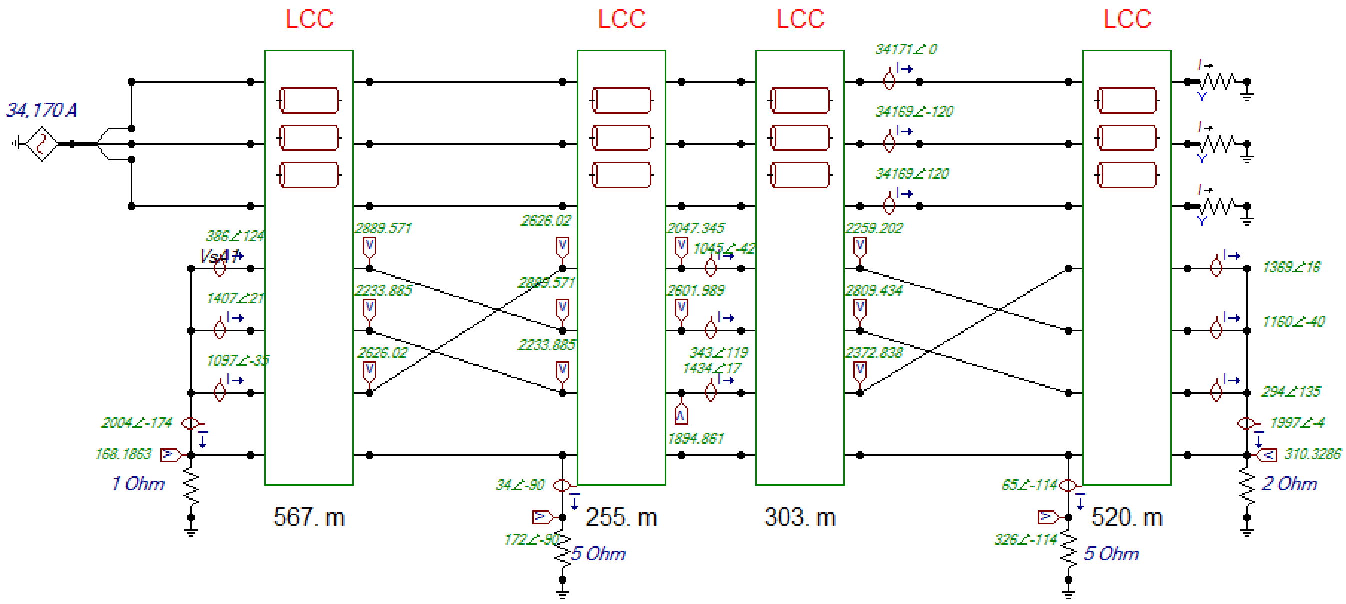

Fig. 16. Simulation model of cable for three phase fault with actual length and cross bonding.

1) Simulation result for cable during normal operation

A single feeder of underground cable system without its neighboring feeders and with multiple feeders in its own duct bank was investigated to observe the influence of magnetic induction from its neighboring feeders. At first, the normal operating current of 100 A was supplied to the observed feeder as load current. The results of induced sheath voltage of each phase for cable formation in duct bank were shown in Figs. 17-18 for with and without neighboring feeders, respectively. The induced sheath voltage was lower than 8 V for a single feeder without neighboring feeders and slightly increased to 9 V for investigation with multiple feeders in its own duct bank. Both results were in acceptable range.

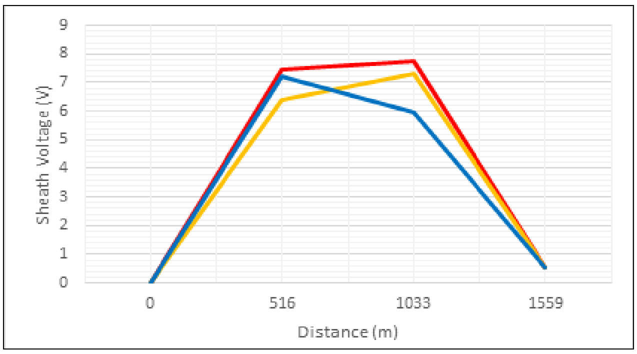

Fig. 17. Induced sheath voltage on a 115 kV single feeder without its neighboring feeders during normal operation.

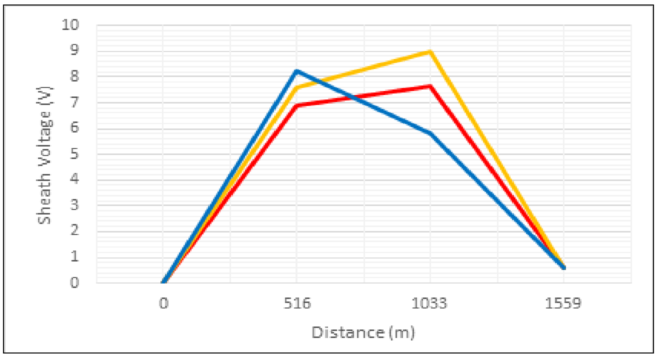

Fig. 18. Induced sheath voltage of a 115 kV single feeder with magnetic induction from its neighboring feeders during normal operation.

2) Simulation result for cable during 3-phase fault.

The 3-phase fault was subsequently studied with this cable feeder. From short circuit study, the fault currents were almost symmetric and balanced as 34.170 kA, which caused the maximum current flowing in the sheath as 1,434 A and 2.37 kV induced voltage drop across cable jacket or between sheath and ground. This 2.37 kV voltage was not relatively large and could be tolerable by cable jacket.

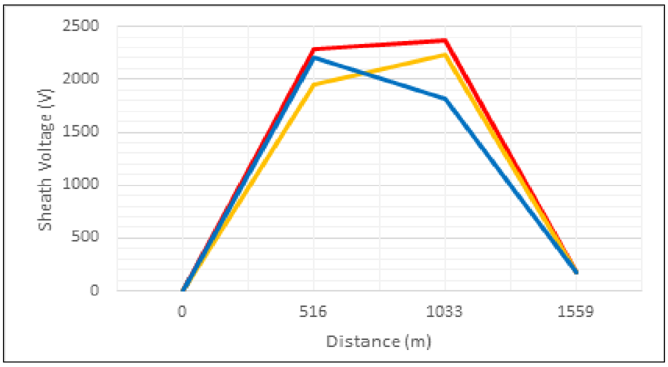

Fig. 19. Sheath voltage on 115 kV cable with 3-phase fault.

3) Simulation result for cable during internal single-line-ground fault

The internal single line to ground fault was modeled as fault within the customer's substation. Similarly from short circuit study, the maximum possible single-line-ground fault current of 32,350 A was fed from generating station via cable to the fault path. The largest current flowing in the sheath was approximately 15 kA for cable modeling without armor. The maximum voltage drop across sheath and ground or cable jacket was around 1.471 kV at cross bonding point of phase-A. The maximum voltage rise of the parallel ground conductor approximately 291 V can be expected.

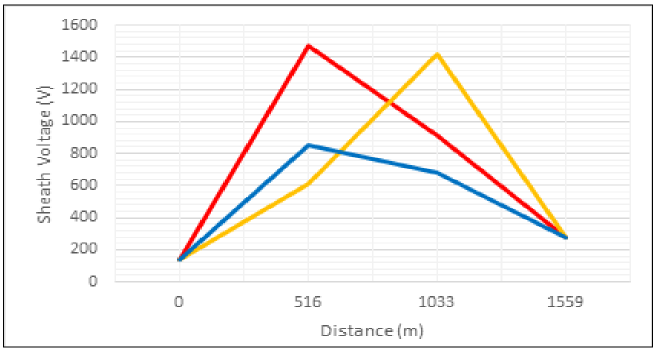

Fig. 20. Sheath voltage on 115 kV cable during internal single line to ground fault.

4) Simulation result for cable during external single-line-ground fault

Finally, the external single-line-ground fault was modeled as fault behind power transformer in the customer's feeders outside the substation. Since a neutral grounding reactance (NGR) was installed to limit the short circuit current, the maximum possible single-line-ground fault current of 1.574 kA was fed to the fault path on the secondary side of power transformer. The majority of fault current returned to the solidly grounded star point of power transformer, while approximately 1 kA current flew through the sheath and approximately 282 A returned to the source of power plant via the parallel ground conductor. The maximum voltage rise of parallel grounded conductor of 291 V can be expected.

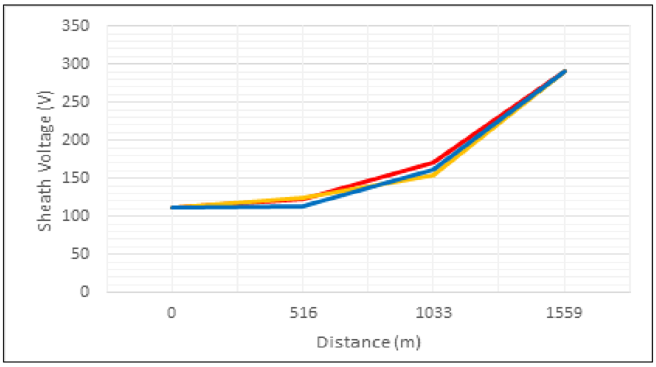

Fig. 21. Sheath voltage on 115 kV cable during external single-line-ground fault.

V. CONCLUSION

The induced sheath voltage and the voltage rise of parallel ground continuity conductor had been investigate with the practical underground cable system. The developed simulation model had been verified with the analytical method according to the international standard. The single point bonding and both-side bonding of single and double feeders of single core cable with cross bonding at joints in the manhole was investigated. The higher the current carrying by a cable leads to the higher induced sheath voltage. However, the magnetic induction of the current flowing in the neighboring feeders had very less impact on the induced sheath voltage. Finally, the abnormal condition in the supply system as three phase and single line to ground faults was investigated. It shows the significant voltage rise between sheath and ground or voltage across cable jacket, which should be carefully considered and controlled to be less than the withstand voltage of the cable jacket. The developed simulation model in ATP/EMTP program was successful and can be further used as a tool for another investigation such as switching transient.

REFERENCES

[1] T. Masuda, T. Morimura, T. Nakano, O. Maruyama, T. Mimura, T. Yasui, K. Agatsuma, and A. Ishiyama, "Safety and Reliability of 66-kV Class HTS Cable Systems in Short-Circuit Current Accidents-Experimental Results on 40-m Cable System," *IEEE Transactions on Applied Superconductivity*, vol. 27 (4), 2017.

[2] H. S. Yang, D. L. Kim, S. H. Sohn, J. H. Lim, H. O. Choi, Y. S. Choi, B. S. Lee, W. M. Jung, H. S. Ryoo, and S. D. Hwang, "Long Term Performance Test of KEPCO HTS Power Cable," *IEEE Transactions on Applied Superconductivity*, vol. 19 (3), 2009.

[3] IEEE Guide for Bonding Shields and heaths of single-Conductor Power Cables Rated 5 kV through 500 kV, IEEE Std 575™-2014.

[4] IEEE Guide for the Application of Sheath-Bonding Methods for Single-Conductor Cables and the Calculation of Induced Voltages and Currents in Cable Sheaths, ANSI/IEEE Std 575- 1988.

[5] J. Angelov, J. Vuletić, R. Ačkovski, and M. Todorovski, "An Extension in Cable Modeling for Grounding System Analysis." *IEEE Transactions on Industry Applications*. vol. 51 (6), 2015.

[6] M. Parol, J. Wasilewski, and J.Jakubowski, "Assessment of Electric Shock Hazard Coming From Earth Continuity Conductors in 110 kV Cable Lines." *IEEE Transactions on Power Delivery*, vol. 35 (2), 2020.

[7] R. Candela, A. Gattuso, M. Mitolo, E. R. Sanseverino, and G. Zizzo, "A Model for Assessing the Magnitude and Distribution of Sheath Currents in Medium and High-Voltage Cable Lines," *IEEE Transactions on Industry Applications*, vol. 56 (6), 2020.

[8] Y. Yang, D. M. Hepburn, C. Zhou, W. Zhou, and Y. Bao, “On-line monitoring of relative dielectric losses in cross-bonded cables using sheath currents,” *IEEE Transactions on Dielectrics and Electrical Insulation*, vol. 24 (5), 2017.

[9] R. Hoerauf, “Ampacity Application Considerations for Underground Cables,” *IEEE Transactions on Industry Applications*, vol. 24 (5), 2017.

[10] IEEE Std 1142-1995. IEEE Guide for the Design, Testing, and Application of Moisture-Impervious, Solid Dielectric, 5-35 kV Power Cable Using Metal-Plastic Laminates, 1995.

[11] IEEE P1617/D3. IEEE Draft Guide for Assessment, Mitigation, and Control of Corrosion of Metallic Shields in Extruded Dielectric Cables rated 5 kV to 46 kV, June 2019.

[12] U. S. Gudmundsdottir, B. Gustavsen, C. L. Bak, and W. Wiechowski, “Field test and simulation of a 400-kV cross-bonded cable system,” *IEEE Transactions on Power Delivery*, vol. 26 (3), 2011.

[13] T. C. Yu, and J. R. Marti, “A robust phase-coordinates frequency-dependent underground cable model (zCable) for the EMTP,” *IEEE Transactions on Power Delivery*, vol. 18 (1), 2003.